29. Yadav, R., Jain, R. K., Dobaria, J. R., Kumar, A., Thirumalaisamy, P. P. and Radhakrishnan, T., Transgenic resistance to *Groundnut bud necrosis virus* (GBNV) in peanut (*Arachishypogaea*L.) plants expressing nucleocapsid protein gene of GBNV. In Proceedings of the 6th International Conference on Legume Genetics and Genomics, Hyderabad, India, 2012.
30. Kunkalikar, S., Marathe, R., Char, B. R., Zehr, U. and Anandlaxmi R., Transgenic approaches for virus resistance in plants. In *Genetically Engineered Crops in Developing Countries* (eds Reddy, D. V. R. *et al*.), Stadium Press, LLC, Houston, USA, 2014, pp. 271–307.
31. Hofgen, R. and Willmitzer, L., Storage of competent cells for *Agrobacterium* transformation. *Nucleic Acids Res*., 1988, **16**, 9877.
32. Wydro, M., Kozubek, E. and Lehmann, P., Optimization of transient *Agrobacterium*-mediated gene expression system in leaves of *Nicotiana benthamiana*. *Acta Biochim. Pol*., 2006, **53**, 289.
33. Bucher, E., Lohuis, D., Van-Poppel, P. M., Geerts-Dimitriadou, C., Goldbach, R. and Prins, M., Multiple virus resistance at a high frequency using a single transgene construct. *J. Gen. Virol*., 2006, **87**, 3697–3701.
34. Yang, C. F., Chen, K. C., Cheng, Y. H., Raja, J. A., Huang, Y. L., Chien, W. C. and Yeh, S. D., Generation of marker-free transgenic plants concurrently resistant to a DNA geminivirus and a RNA tospovirus. *Sci. Rep*., 2014, **4**, 5717.

ACKNOWLEDGEMENTS. The doctoral fellowship to S.K.H. by the PG School IARI, New Delhi is gratefully acknowledged. This research was funded by Department of Biotechnology (DBT), New Delhi (Grant no. BT/PR7866/AGR/02/379/2006) and NAIP Component-4 (ICAR-World Bank) subproject – Novel strategies for molecular diagnosis of plant viruses.

Received 15 May 2017; revised accepted 23 November 2017

doi: 10.18520/cs/v114/i08/1742-1747

Dual transmitter–receiver electromagnetic system for lateral boundary detection of subsurface formations

R. Rajesh* and V. S. Sarma

CSIR-National Geophysical Research Institute, Uppal Road, Hyderabad 500 007, India

A new frequency domain electromagnetic system, based on different working principle has been designed and its efficacy tested over the existing systems through laboratory-scale-model studies. In this system, two transmitter coils have been employed to generate a magnetic null plane at their geometric centre. The receiver coil is placed in the null plane to record the induced secondary field. The interaction of the primary field is almost negligible on the secondary field recorded by the receiver. We present the theory and physical model results describing the system parameters and efficacy. The testing through physical model studies suggests an increased depth of detection in this new configuration compared to the existing systems. In terms of secondary field, the strength of the anomaly reflects the magnetic permeability/susceptibility difference of the subsurface medium on either side of the receiver. The study concludes that there is significant increase in depth of investigation and secondary field strength in this system over the existing conventional frequency domain systems and also more robust for boundary detection.

Keywords: Conducting bodies, electromagnetic system, magnetic permeability, physical model studies, susceptibility.

ELECTROMAGNETIC (EM) methods are popular for a wide variety of applications in exploring the internal structure of objects by transmitting the primary electromagnetic field and analysing the induced secondary field intensities. Similar mechanism is involved in the geophysical electromagnetic exploration for measuring conductivity/susceptibility of the subsurface formations to map the mineral/ore deposits[1]. Geometrical electromagnetic sounding is a popular technique, in which the separation between the transmitter and receiver coils is increased to achieve deeper penetration[2]. The skin depth is the most important and interesting phenomenon that restricts the penetration of the fixed frequency electromagnetic energy up to a constant depth for a fixed transmitter (Tx) and receiver (Rx) separation within a subsurface layer with specific electrical conductivity[3,4]. Most of the frequency domain electromagnetic systems utilize the concept of skin depth to scan the subsurface by decreasing the frequency of the primary field. Such frequency sounding is the most popular method since the past five decades in geophysical electromagnetic exploration[5]. These systems are handy in near subsurface study, such as groundwater exploration in hard-rock terrains, soil pollution study, mineral exploration, etc.

Different techniques and coil configurations have been developed to nullify the influence of strong primary field on the receiver in frequency domain EM exploration. Recently, researchers have designed the vertical primary decoupled coil configuration (VPDCc) to nullify the effect of primary field on the receiver[6,7]. They have suggested placing the receiver coil at a strategic position where the primary magnetic field horizontal component is zero. The performance and stability of VPDCc have been tested and found efficient among the existing conventional coil configurations using laboratory studies. However, the complicated non-coplanar and non-coaxial geometrical set-up of the transmitter and receiver coils in the VPDCc reduces its wider applicability.

*For correspondence. (e-mail: rekapalli@gmail.com)

In this communication, we present a new frequency domain electromagnetic system known as 'dual transmitter receiver electromagnetic (DuTrEM)' system. We discuss the working principle and its theoretical background. Then we provide the results on testing of the DuTrEM system over conducting targets of different geometries using a laboratory model in comparison with VPDCc.

The DuTrEM system employs two transmitters and one receiver with vertical co-axial configuration. The problems with the VPDCc geometry are circumvent with the new configuration in which three coils are engaged coaxially. The centre coil works as the receiver and the two other are the transmitters placed at equal distances on either side of the receiver. The two transmitters produce electromagnetic dipole fields with opposite directions to generate a magnetic cavity plane between them by sending current in opposite directions. It is known from the basic properties of magnetism that the like poles repel each other. Therefore, generation of the magnetic null plane could be possible if the two coils produce opposite magnetic fields. The repulsion between magnetic field lines of force allows deep penetration of the field to incorporate more depth of investigation. The null plane will be at the geometric centre if both the two transmitter coils possess the same parameters (number of turns, radius, thickness and the current sent). Figure 1 *a* shows a schematic diagram of the proposed configuration. The receiver coil is placed coaxially in this magnetic null plane to pick up only the secondary induced anomaly field arising due to the difference in the electromagnetic properties (conductivity, magnetic permeability and electrical permittivity) of the subsurface on either side of the receiver. Figure 1 *b* shows the magnetic field distribution pattern of the DuTrEM system.

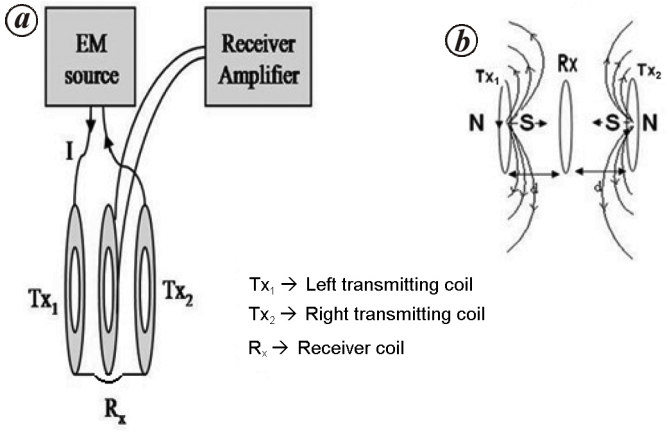

Figure 1. (***a***) Block diagram and (***b***) schematic magnetic field diagram of dual transmitter electromagnetic (DuTrEM) system.

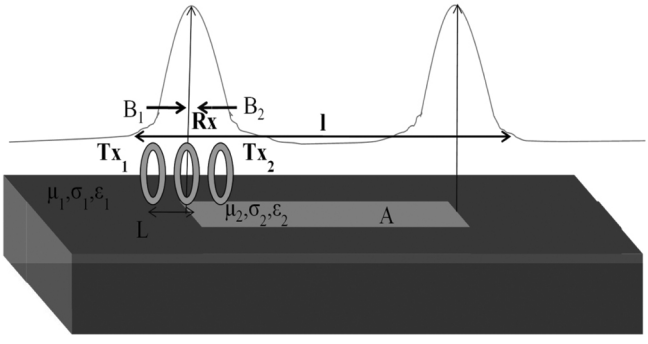

Figure 2. Model anomaly cure over an outcropped embedded formation within homogeneous medium. $A \rightarrow$ Formation with electromagnetic properties μ_2, σ_2, ε_2 embedded within an homogeneous medium with properties μ_1, σ_1, ε_1. $B_1 \rightarrow$ Mangetic field induced in the formation of length l with properties μ_1, σ_1, ε_1. $B_2 \rightarrow$ Magnetic field induced in the formation with properties μ_2, σ_2, ε_2. $L \rightarrow$ Transmitter–receiver separation.

The equation for resultant magnetic field at the receiver due to the two transmitters is simply the vector sum of two magnetic fields from the transmitters. The induced voltage in the receiver coil is proportional to time-varying magnetic field at the receiver. The equation for the magnetic field at the receiver coil in terms of magnetic permeability/susceptibility can be obtained as follows.

Let us suppose that the system is placed on the surface and imagine that the boundary between the formations falls exactly beneath the receiver, as shown in Figure 2. Now, the voltage induced in the receiver is due to the resultant induced magnetic field from the two transmitters at the receiver. The magnetic field at the receiver due to the first transmitter (Tx_1) is given by (assuming that the coils contain only one turn).

$$\mathbf{B}_1 = \frac{\mu_1 2\pi a^2}{4\pi (l^2 + a^2)^{3/2}} \mathbf{I}. \tag{1}$$

Similarly, the magnetic field at the receiver due to the second transmitter (Tx_2) is

$$\mathbf{B}_2 = \frac{\mu_2 2\pi a^2}{4\pi (l^2 + a^2)^{3/2}} \mathbf{I}. \tag{2}$$

So, the net magnetic flux through the receiver is

$$\Delta\mathbf{B} = \frac{(\mu_1 - \mu_2) \cdot 2\pi a^2}{4\pi (l^2 + a^2)^{3/2}} \cdot \mathbf{I} \tag{3}$$

or

$$\Delta\mathbf{B} = \frac{(\chi_1 - \chi_2) \cdot 2\pi a^2}{4\pi (l^2 + a^2)^{3/2}}. \tag{4}$$

Here μ_1 and μ_2 denote the magnetic permeability of the homogenous medium and formation 'A', and χ_1 and χ_2 denote the magnetic susceptibilities of the homogenous

medium and formation 'A' respectively (Figure 2). a is the radius of the transmitter and receiver coils and l is the separation between the transmitter and receiver coils.

The difference in the magnetic properties of the medium produces an induced residual time-varying magnetic field following eqs (3) and (4). The receiver coil converts the residual induced magnetic field to voltage and will be measured using an appropriate device. This voltage is therefore a measure of the induced electromagnetic field difference from the subsurface material on either side of the receivers.

Figure 3 shows the DuTrEM system set-up in the laboratory to conduct scale model studies over targets with different transition parameters. In the present study, copper wire of 1 mm gauge is used for winding the coils (transmitter as well as receiver). Each coil contains 150 turns with an average radius of 2.5 cm. We have utilized basic operational amplifier UA741 in the receiver amplifier and modified TDA2030 dual-channel audio power amplifier as transmitter. The system is driven by 18 W power amplifier in the frequency range 10–100 kHz. An amplifier with gain-2 has been employed in the receiver circuit. As the anomaly is normalized, the gain of the receiver amplifier will not affect data analysis and interpretation. In the ideal case, the receiver output voltage of the system over homogeneous medium will be zero. However, due to practical limitations in maintaining equal separation between the receiver and transmitter coils at micro level to achieve exact magnetic null plane, we consider 10–20 mV as zero receiver anomalies. The system calibration/null-field adjustment can be done as follows.

The receiver coil will be fixed at the centre and the transmitters on either side are flexible to move along the axis. The system has to be calibrated at the particular frequency of interest within a reference medium by slightly adjusting the separation between the receiver and one transmitter while keeping the other transmitter at a particular distance, until the receiver voltage between ~0 and 20 mV is achieved. This is called 'magnetic null set-up' or simply 'null set-up'. Once the system is calibrated for null set-up, we can proceed to acquire the data. If one wants to go for a wide range of frequency, it is suggested to calibrate the system for each frequency separately.

Profiling data over a vertical graphite sheet of thickness 5 mm, length 750 mm and breadth 400 mm are obtained using both VPDC and DuTrEM configurations for different target depths (d) in a model tank made up of non-conductive material within the host medium of free space using Tx_1–Rx–Tx_2 separation of 5 cm. The target is kept at a horizontal distance 40 cm from the starting point of the profile (i.e. 0 cm in Figures 4 and 5). Figures 4 and 5 show the percentage of anomaly calculated for the vertical graphite sheet at different depths using both the systems. As VPDCc was proven as a more efficient system over conventional horizontal co-planar (HCP) configuration, we have compared the DuTrEM configuration with

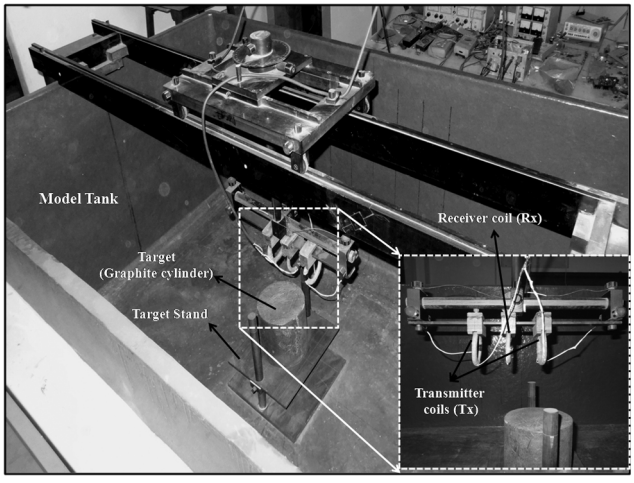

Figure 3. Laboratory set-up of DuTrEM system.

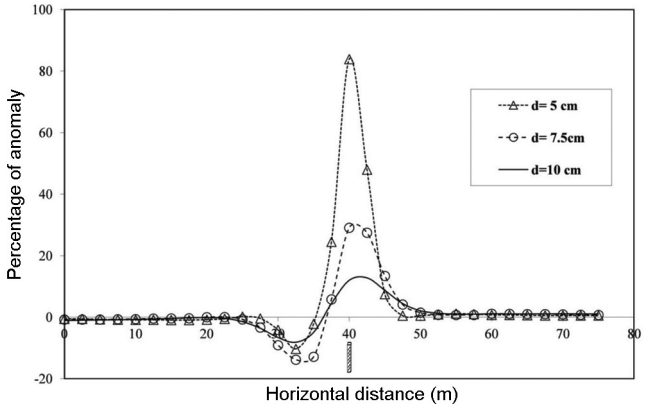

Figure 4. Percentage of anomaly observed over a vertical graphite sheet (l = 750 mm, b = 400 mm, t = 5 mm, f = 60 kHz, Tx–Rx separation L = 50 mm) using DuTrEM configuration. Target is placed at a horizontal distance of 40 cm.

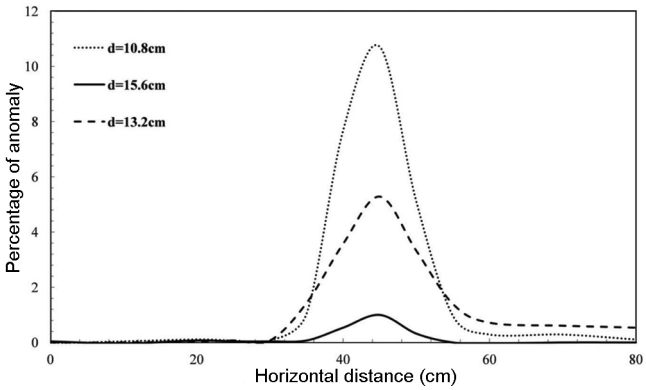

Figure 5. Percentage of anomaly observed over a vertical graphite sheet (l = 750 mm, b = 400 mm, t = 5 mm, f = 60 kHz, Tx–Rx separation L = 100 mm) using vertical primary decoupled coil configuration. Target is placed at a horizontal distance 40 cm.

Table 1. Comparison of percentage of anomaly over a vertical graphite sheet (l = 750 mm, b = 400 mm, t = 5 mm) using vertical primary decoupled coil configuration and dual transmitter–receiver electromagnetic configurations

Configuration	Target depth (h cm)	Tx–Rx separation L (cm)	Frequency (kHz)	h/L	Percentage of anomaly
VPDCc	10.8	12	60	0.9	10
VPDCc	13.2	12	60	1.1	5.2
VPDCc	15.6	12	60	1.3	1.2
DuTrEM	5	5	60	1	88
DuTrEM	7.5	5	60	1.5	30
DuTrEM	10	5	60	2	12

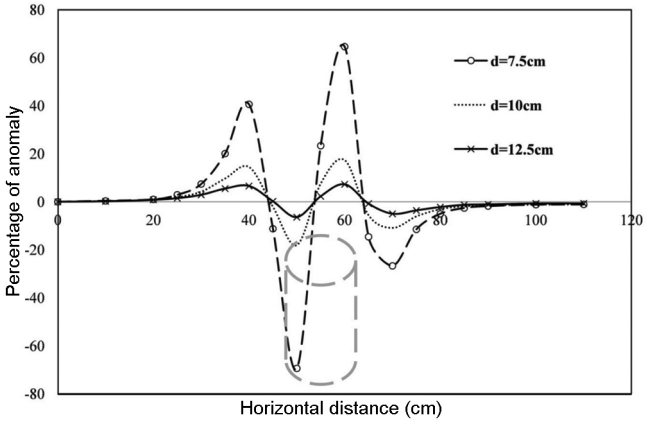

Figure 6. Percentage of anomaly obtained over a vertical graphite cylinder (L = 150 mm, r = 75 mm) for different target depths using Tx–Rx separation of 50 mm and frequency 50 kHz at different depths (d = 75, 100 and 125 mm). Target is placed at a horizontal distance of 55 cm.

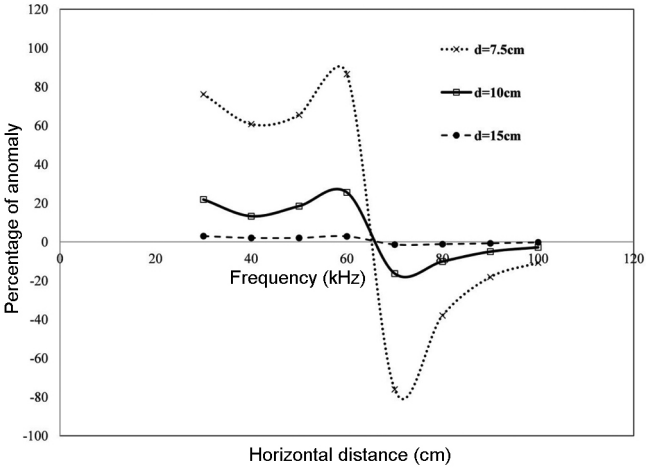

Figure 7. Frequency response of DuTrEM over a graphite cylinder (L = 150 mm, r = 75 mm) for different target depths (T_d = 7.5, 10 and 15 cm) using Tx–Rx separation of 5 cm. Target is placed at a horizontal distance of 55 cm.

VPDCc to verify its efficacy in terms of percentage of anomaly for different target depths. Table 1 provides a comparison of the percentage of anomaly observed from both the systems for the same transition parameters. It can be observed that the strength of the anomaly with DuTrEM for the same h/L ratio is almost eight times higher than VPDCc. Figure 6 shows the profiles over a vertical graphite cylinder for different target depths. Our results indicate that the anomaly obtained over the graphite cylinder (65%) is almost double that over the vertical sheet (30%) for h/L ratio of 1.5. The high anomaly percentage justifies the larger volumetric contribution of the solid graphite cylinder compared to the thin vertical sheet.

Further, frequency response of the system has been studied to verify the frequency stability in laboratory scale. Figure 7 depicts the profiling anomalies over a vertical graphite cylinder of length 16 cm and diameter 15 cm at different depths using frequencies between 30 and 100 kHz with Tx–Rx separation of 5 cm. From the frequency response it is clear that the system can be operated in the frequency range 10–80 kHz to detect targets at depths up to 1.8 times to the Tx–Rx separation with conductivities less than or equal to that of graphite. With more accurate instrumentation amplifiers and power amplifiers, one can achieve better results using DuTrEM configuration.

Finally we have obtained profiles over a horizontal aluminium sheet (l = 60 cm, b = 25 cm, t = 0.2 cm) along its breadth to verify the system applicability on other conducting materials as well as its efficacy in measuring the extension of the conducting body. Figure 8 depicts the anomaly curve for different depths (10, 15 and 20 cm) over the aluminium sheet using Tx–Rx separation of 7.5 cm. Even though the sheet is very thin, it is possible to detect the target up to a depth approximately equal to twice the Tx–Rx separation. The boundaries of the aluminium sheet are clearly identified by the peaks of the anomaly curve. The distance between the two peaks is 25 cm, which is exactly equal to the physical breadth of target. As the conductivity of aluminium is higher than that of graphite, the strength of the anomaly is high in case of thin aluminium sheets compared to graphite sheets. From the physical model studies it is observed that the new system provides more depth of investigation and accurate boundary detection compared to conventional systems. The improved depth of investigation is

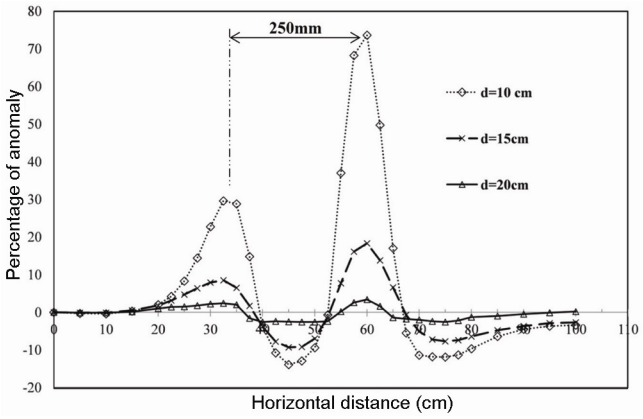

Figure 8. Percentage of anomaly observed over a thin horizontal aluminium sheet (l = 600 mm, b = 250 mm, t = 2 mm, f = 40 kHz and Tx–Rx separation L = 75 mm) for target depths d = 100, 150 and 200 mm.

possible because of the repulsion between the magnetic lines of force. The depth of investigation is 1.8 times the Tx–Rx separation, and the strength of the anomaly is eight times more compared to the VPDCc system.

We have designed and developed a new frequency domain electromagnetic system for geophysical exploration of subsurface conductive bodies. The physical model laboratory studies over conducting bodies with different transition parameters show that this configuration is efficient compared to the conventional frequency domain systems. The system facilitates accurate boundary detection between geological formations with different electrical properties. The proposed system can be operated over a wide range of frequencies to scan the subsurface with high resolution. The main features of the system are as follows: (i) depth of investigation of the system is around ~1.8 times the transmitter–receiver separation and the strength of the anomaly is eight times more compared to the VPDCc system. (ii) As the receiver is placed in the magnetic null plane, the observed anomaly is directly proportional to the difference in the magnetic properties between the subsurface lateral extents and provides accurate boundary detection. (iii) The exact estimation of the target length/breadth is possible as the boundaries between the different formations are clearly indicated by peaks in the anomaly curve.

1. Huang, H. and Won, I., Conductivity and susceptibility mapping using broadband electromagnetic sensors. *J. Environ. Eng. Geophys.*, 2000, **5**(4), 31–41.
2. Spies, B. R., Depth of exploration in electromagnetic sounding methods. *Geophysics*, 1989, **54**, 872–888.
3. Huang, H., Depth of investigation for small broadband electromagnetic sensors. *Geophysics*, 2005, **70**(6), G135–G142.
4. Singh, N. P. and Mogi, T., Effective skin depth of EM fields due to large circular loop and electric dipole sources. *Earth Planets Space*, 2003, **55**, 301–313.
5. Duckworth, K. and Krebes, E. S., Depth sounding by means of a coincident coil frequency domain electromagnetic system. *Geophysics*, 1998, **62**, 49–55.
6. Gupta, O., Rao, S. and Joshi, M., Moving source dipole electromagnetic exploration device for deeper and poorer conductors and a method of detecting such conductors, US Patent, 2004; https://www.google.com/patents/US20040000919
7. Nageswararao, S. and Gupta, O. P., An electromagnetic moving source system for detection of subsurface mineralized zones. *Curr. Sci.*, 2007, **92**(1), 110–113.

ACKNOWLEDGEMENTS. We thank the Director, CSIR-NGRI, Hyderabad for encouragement. R.R. thanks CSIR, New Delhi for funds.

Received 23 August 2017; revised accepted 13 November 2017

doi: 10.18520/cs/v114/i08/1747-1751

Overestimated groundwater ^{14}C ages triggered an inexpediency of water policy in China

Tao Wang[1,2] and Jiansheng Chen[1,*]

[1]Geotechnical Research Institute, College of Civil and Transportation Engineering, Hohai University, Nanjing 210098, China
[2]College of Hydrology and Water Sources, Hohai University, Nanjing 210098, China

Northern China has been facing a serious problem of groundwater scarcity. The government developed restrictive policies on groundwater extraction, and designed the South–North Water Transfer Project (SNWTP) to transfer water from the Yangtze River in southern China to the arid region in the north. However, contrary to expectation, groundwater levels in northern China have been rising significantly before completion of the project. Due to misapplication of the ^{14}C dating method, the age of deep confined groundwater in arid northern China has been overestimated. This classifies the groundwater as palaeo-groundwater with little recharge, which results in the prohibition of groundwater extraction and SNWTP. Significant tritium concentrations recently reported in the so-called palaeo-groundwater, along with rising groundwater levels, imply recent groundwater recharge in arid northern China.

Keywords: Groundwater, ^{14}C dating method, northern China, South–North Water Transfer Project.

THE problem of groundwater scarcity in northern China is very severe than any other parts of the world[1–3]. In the 1980s and 1990s, long-term over-exploitation of groundwater resulted in sustained lowering of groundwater

*For correspondence. (e-mail: jschen@hhu.edu.cn)